Global NEST Journal, Vol 24, No 3, pp 526-536

Turbidity reduction of groundwater by using nanomagnetic adsorbent composite (NMAC): Process optimization by 3^k factorial design and analysis

Awang H[1], Abdullah N.A.[1], Barasarathi J.[2], Ling H.Y.[1], Wen L.K.[1], Nadhirah H.[1], Azmin S.N.H.M.[1], and Abdullah P.S.[1*]
[1]Faculty of Agro-Based Industry, Universiti Malaysia Kelantan Jeli Campus 17600 Jeli, Kelantan, Malaysia
[1]Faculty of Health and Life Sciences, Inti International University, Nilai, Negeri Sembilan, Malaysia
Received: 12/05/2020, Accepted: 01/09/2022, Available online: 26/09/2022
*to whom all correspondence should be addressed: e-mail: palsan.abdullah@umk.edu.my
https://doi.org/10.30955/gnj.003343

Graphical abstract

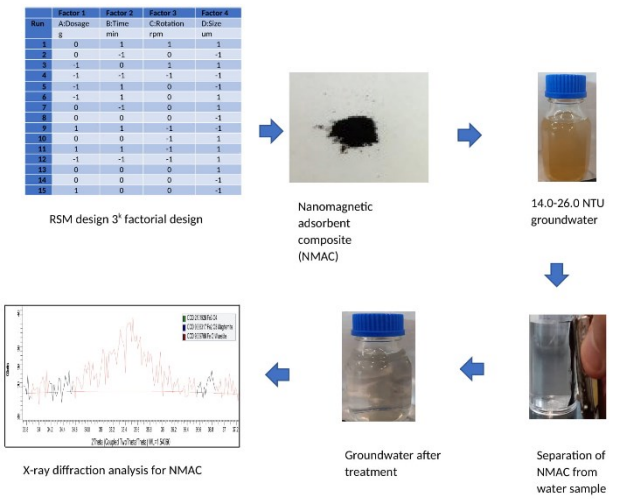

Abstract

The widespread use of alternative water sources in Kelantan encourages the development of cost-effective methods for the purification of water. A simple and straightforward adsorption process using a nanomagnetic adsorption composite (NMAC) was introduced in this study as a new adsorbent for the treatment of turbid polluted groundwater. The use of iron oxide nano-coated adsorbents (NMACs) showed a high porosity relative to commercial activated carbons (CACs). Analysis of X-ray diffraction analysis for NMAC is confirmed by a crystal framework for Fe_2O_3, Fe_3O_4, and FeO are cubic components. A 3^k maximum factor configuration of four factors, i.e., adsorbent dosage (0.02, 0.04, and 0.06 g), agitation time (15, 30, and 60 min), rotation speed (150, 200, and 250 rpm) and adsorbent scale (< 45 µm and >300µm) were used. The turbidity removal capability of both NMAC and CAC was compared. The adequacy of the developed empirical model for the elimination of turbidity and maximum turbidity efficiency was determined by regression model analysis. The obtained results revealed regression values of NMAC (R^2; 0.9903, R^2 adj.; 0.9875, R^2 pred; 0.9808) and CAC (R^2; 0.9909, R^2 adj.; 0.9981, R^2 pred.; 0.9817). The analysis of variance and surface response methodology revealed that turbidity removal efficiency of NMAC is affected by the four factors investigated. Among the samples, 0.04 g NMAC (< 45 µm) agitated at 150 rpm for 48 min showed 98.76% maximum adsorption efficiency. The findings showed that NMAC is a strong adsorbent for use in the treatment of raw water.

Keywords

Activated carbon, adsorbent, factorial design, nanomagnetic composite, turbidity, wastewater

1. Introduction

The use of groundwater is still common among Malaysians, especially at east coast of peninsular Malaysia, Kelantan and about 38% of the population in the State of Kelantan use groundwater for consumption (Ayob *et al.,* 2022). Residents in the northern part of Kelantan are taking advantage of the aquifer for consuming groundwater at a high rate (4.22±0.17 mm/year) (Yong *et al.,* 2018). The rapid growth of the population and accelerated urbanization raises demand for groundwater consumption. Groundwater provides half of all water used by households worldwide, a quarter of all the water drawn for irrigated agriculture, and one third of the water supply required for industry (WHO, 2022). Improper disposal of wastewater coming from municipal and agricultural sources with little to no treatment before discharge is considered a common practice, and this has led to the eventual leaching of contaminants into the soil, which causes the significant depletion of groundwater quality (Zainol *et al.,* 2021) and furthermore mproper waste management among industry operators and excavation that exceeds the groundwater aquifer level leads to turbidity problem with groundwater (Mohd Faiz & Noorazuan, 2018). A preliminary study conducted at Tanah Merah, Pasir Mas, and Jeli revealed that turbidity reading (>5 NTU) of samples from tube well exceeded the Drinking Water Quality Standard (Minister of

Health, 2012; Huda *et al.,* 2020; Huda *et al.,* 2022). There are different methods applied to overcome the problem, including coagulation, flocculation, and membrane filtration (Park *et al.,* 2020). The formation of turbidity in water is due to the decomposition of organic matter by soil microorganisms known as humus, and the presence of peat soil with high iron content (Hazimah *et al.,* 2019). The presence of turbidity in groundwater not only reduces the aesthetic quality of the water but is also associated with gastrointestinal acid reflux disease among consumers (Muoio *et al.,* 2020). The use of poly aluminum chloride (PAC) coagulant is able to decrease residual turbidity to below 1.0 NTU. However, the drawback of coagulation is the removal of dissolved organic matter (Liu *et al.,* 2018). Adsorption is one of the more preferred conventional cleanup methods applied by industries for water treatment. Adsorption has commonly been opted for water treatment not only due to its simplicity but also for its performance. The adsorption process most likely involves physical rather than chemical phenomenon because a stable molecular surface complex will form at the interface during adsorption (Crini *et al.,* 2018). Powdered activated carbon (PAC) is widely used as adsorbent due to its high surface area and adsorption capacity. However, the recovery process for the spent powdered activated carbon through a gravitational separation is challenging due to small particle size, therefore increasing costs for treatment (Meng *et al.,* 2019). Iron oxide nanomaterial called hematite (α-Fe_2O_3) is magnetic, with lower operation costs, higher adsorption property, and environmentally friendly (Santosh *et al.,* 2019). Although hematite (α-Fe_2O_3) particles self-aggregate during adsorption, modification of its surface by anchoring the particles onto organic molecules can overcome the problem (Tancredi *et al.,* 2019). The innovation had been done by tailoring the iron oxide nanoparticles on powdered activated carbon known as nanomagnetic adsorbent composite (NMAC). The adsorption of copper (Cu^{2+}) by NMAC showed 88% removal efficiency (Wannahari *et al.,* 2018). Therefore, the innovation improves not only adsorption activity but also the recovery of the NMAC from solution by applying an external magnetic field (Wannahari *et al.,* 2018). However, the NMAC efficiency in removing turbidity from raw water has not been tested yet. It is critical to remove turbidity in groundwater with Malaysia Drinking Water Standard (below 5 NTU) compliance. Apart of that, application of agricultural waste as source for biodegradable adsorbent is getting attention among researchers due to potential of competing commercial activated carbon (Basrur & Ishwara, 2019). Thus, agricultural waste was utilized to develop adsorbent components for NMAC (Wannahari *et al.,* 2018). The addressed challenges for NMAC include recovering the NMAC in the separation process and competing for commercial activated carbon (CAC). Therefore, the optimization of NMAC adsorption was conducted by adopting a 3^k factorial design. Four factors were considered, including dosage of adsorbent, size of adsorbent, rotation speed, and time for agitation with three levels for each factor. In this study, significant factors and interactions were identified, while the opti-mum levels of the variables increase removal efficiency.

2. Materials and methods

2.1. Chemicals

All reagents used for the iodine number tests are of analytical grade. An iodine solution (0.1 N) was prepared from iodine pearl (Friendemann Schmidt Chemical) and potassium iodide (KI; Friendemann Schmidt Chemical) with iodine-to-iodide weight ratio 1:1.5. A 0.1 N sodium thiosulphate pentahydrate ($Na_2S_2O_3.5H_2O$; Friendemann Schmidt Chemical) was prepared with 0.1 g sodium carbonate (Na_2CO_3). A 10 % starch solution was used during titration.

2.2. Preparation and characterization of adsorbate

All of NMAC preparation steps were adapted from Wannahari *et al.,* (2018). To begin with, coconut shell (CS) went through pyrolysis process to produce powdered carbonized CS prior to potassium hydroxide (KOH) activation process with slow agitation for 5 to 6 h. Then, the activated coconut shell (ACS) was filtered, rinsed with distilled water, and dried in an oven at 100 °C. Later, the sample continued drying process in a muffle furnace (Carbolite ELF 11/6B) at range 800-900 °C with rate (10 °C/min). The dried sample was cooled down for 30 minutes before washing and treating with 5%HCl. The treated ACS sample was dried again in an oven 100 °C and treated with nitric acid (HNO_3) solution for 1 h at 80 °C.

Reaction solution was prepared by using mechanical stirring for dissolving $FeCl_3.6H_2O$ and $FeSO_4.7H_2O$ in 450 mL of deionized water for 30 min at 30 °C. Next, 30-60 mL of ammonium hydroxide ($NH_3.H_2O$) solution was mixed vigorously at 70 °C for 1 h to form precipitate. Later, 5 g of the prepared ACS sample in previous stage was mixed into the reaction solution followed by addition of 6 mL epichlorohydrin and continued stirring process at 85 °C for 1 h. Sonication (Q sonica) of reaction mixture took place at 80 λ for 1 h by using. Upon completion of sonication, stirring process was continued for 1h at 85 °C. Then, the synthesized NMAC was cooled down at 27° C, washed with deionized water and ethanol, test for pH and dried for 48 h at 50 °C. The NMAC was sieved accordingly (<45 µm) and (>300 µm) and ready for application.

The CAC was also washed, neutralized, dried, and sieved accordingly.

2.2.1. Proximate analysis

Proximate analysis to determine the volatile matter, moisture, ash, and fixed carbon content of the respective adsorbate was conducted as per procedure (Milne *et al.,* 1992). The iodine number determination was carried out by adopting the standard method for activated carbon (ASTM, 2006).

2.2.2. Surface characterization of NMAC

The Brunauer-Emmett-Teller (BET) analysis was performed to identify total pore volume (m^3/g), average pore volume (nm), and BET surface area (m^2/g) by using a QuantachromeAutosorb iQ3 Automated Gas Sorption

Analyzer (Quantachrome Instruments, US) at 77K. Analysis of crystalline structures (iron oxide nanomaterials) of NMAC was carried out through X-ray diffraction analysis (XRD; Bruker, D8 Advance X-RD) aided by Diffract Plus Eva Software for crystalline state detection. The analyses were conducted at room temperature with the following conditions; uncoated samples used, CuKα radiation (λ = 1.5406 Å) in the 0.01% s range started at 2θ: 5° to 90°. Measurement for the size of particle was carried out in a Zetasizer nano series ver. 7.03 (Malvern Ltd). Meanwhile, observation for morphology and elemental analysis was performed through JEOL SEM/EDX (JSM 6400) instrument with 15 kV.

2.3. Water sampling

The turbid groundwater was taken from a local well in Tanah Merah, Kelantan (coordinates: N 5° 4856.8 E 102° 0757.1. The initial turbidity of this raw water was approximately 23NTU.

2.4. Batch adsorption studies

The adsorption study was conducted by batch method with 10% adsorbent in the working volume. The parameters tested for the adsorption were the size of adsorbent, dosage of adsorbent, rotation speed, and time of agitation. The test adsorbent was NMAC, while CAC was the reference. The percentage of turbidity removal was calculated as in Eq. 1.

$$Percentage\ of\ turbidity\ removal = \frac{NTUi - NTUe}{NTUi} \times 100 \qquad (1)$$

NTU_i =Initial NTU reading

NTU_e = Residual NTU reading at equilibrium

2.5. Analytical method for groundwater sample

The turbidity of groundwater was measured by using turbidity meter with a fast tracker (Hanna Instruments, Romania).

2.6. Statistical analysis

In order to study the removal of turbidity responses to variation in parameters, the 3-Factorial design is used by the application of Response Surface Methodology (RSM) approach. The strategies in this method are; design of experiments (DOE) to evaluate model parameters after conducting experiments and develop second-order polynomial (Eq. 2) based on the obtained responses (Tezcan *et al.,* 2015).

$$y = \beta_0 + \sum_{i=1}^{k} \beta ijxi + \sum_{i=1}^{k} \beta ijx^2 i + \sum\sum_{i<j=2}^{k} \beta ijxixj + \varepsilon \qquad (2)$$

The equation consisted of predicted response (y), the number of factors (k), constant (β_0), ith linear coefficient (β_i), ith quadratic coefficient (β_{ij}), ith interaction coefficient (β_{ij}), the independent variable (x_i), and error (ε).

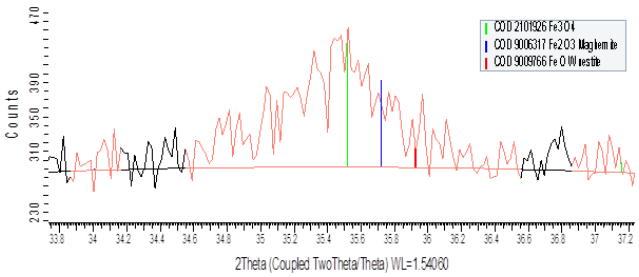

Figure 1. Intense peaks that indicated the presence of Fe_2O_3, Fe_3O_4, and FeO at 2θ peaks of 35.522°, 35.721°, and 35.928° respectively.

In this study, the 3k factorial design for numerical factors consisted of dosage, agitation time, and rotation speed denoted as A, B, and C. Meanwhile the categorical factor involved the size of the adsorbent denoted as D. The levels of each factor were coded as -1 (low), 0 (middle), and 1 (high) as in Table 1.

Numerical considerations differed with an additional six center points on 27 different treatments, so cumulative runs totaled to 33 (n=33). Since the design involves a two-level categorical element, this experiment was duplicated with up to 66 total runs (n=66). The percentage of removal efficiency was used as response of treatments combinations. An empirical model was generated after handling the response of each combination. The calculation of fitting values and checking the adequacy of the model, was carried out. The analysis of variance (ANOVA) for each factor was adopted by using Design Expert ver. 11. An optimization with verification process was conducted to test the reliability of the generated empirical model.

Table 1. Input factors for 3k factorial design and their levels

Types of factors	Factors	Unit	Symbol	Levels		
				-1	0	1
Numerical	Dosage of adsorbent	g	A	0.02	0.04	0.06
	Time of agitation	min	B	15	30	60
	Rotation speed	rpm	C	150	200	250
Categorical	Size of adsorbent	µm	D	<45		>300

3. Results and discussion

3.1. Characterization of adsorbent composites

3.1.1. Proximate analyses

The results of proximate analyses (Table 2) show that NMAC possesses higher moisture content, ash content, and fixed carbon compared to CAC. The moisture content of NMAC is higher than CAC because of the moisture adsorbing nature of the carbonate group, and the iron oxide nanoparticles found in NMAC pores; a similar finding reported by Karthikeyan *et al.* (2008). Ash contents are minerals residue such as magnesium, calcium, and sodium in the pore of activated carbon (Zulkarnia *et al.,* 2018). NMAC has higher ash contents in comparison to CAC, so it is undesirable as it might reduce the mechanical strength of carbon for adsorption (Hidayu *et al.,* 2013). Besides, a

low percentage of volatile matter indicates that the pore structure of NMAC is porous and rigid as opposed to CAC (Hidayu *et al.,* 2013). Iodine number test was conducted to identify the porosity of the adsorbent. The BET analysis showed total pore volume, BET surface, and average pore volume of NMAC were 0.67 m^3/g, 916.19 m^2/g, and 14.6 nm compared to CAC (0.46 m^3/g, 769.50 m^2/g, and 20.53 nm). Based on the obtained result, the porosity of NMAC is higher than CAC. The presence of iron oxide nanomaterial increases the porosity of NMAC. Therefore, NMAC can be an efficient adsorbent in terms of surface areas, and pore volumes of porous material are vital factors for high-performance adsorption (Sun *et al.,* 2019).

3.1.2. Characterization of nanomagnetic adsorbent composite (NMAC)

Iron oxide nanomaterials not only increase porosity but also contribute to magnetic property on the adsorbent. The presence of Fe_2O_3, Fe_3O_4, and FeO in the diffraction peaks characteristics of XRD patterns indicate the existence of magnetic microcrystalline on NMAC. The spectrum reading determined the presence of Fe_2O_3, Fe_3O_4, and FeO by peak observed at 35.522°, 35.721°, and 35.928°, respectively. Based on the analysis, as in Figure 1, the crystalline system structure of the composite is cubic. The present findings seem to agree with another research by Zhu (2018) reveals that the occurrence of nanomagnetic particles for peaks at 2θ (Fe_3O_4) are 30.22°, 35.62°, 57.50° and 62.42° which was used for the synthesis of bamboo biochar coated with α-Fe_2O_3 / Fe_3O_3 through impregnation of ferric solution.

Table 2. Comparison of proximate analysis between NMAC and CAC

Parameter	NMAC	CAC
Moisture content (%)	3.71	2.75
Ash content (%)	22.96	20.27
Volatile (%)	13.52	19.77
Fixed carbon (%)	59.81	57.10
Iodine number	913.50	869.10

Table 3. Codified variables and responses obtained for turbidity removal by NMAC and CAC

	Variables				Responses	
Run	A: Dosage of adsorbent	B: Time of agitation	C: Rotation speed	D: Size of adsorbent	Removal	Efficiency (%)
	g	min	rpm	um	NMAC	CAC
1	-1	-1	-1	-1	93.69	83.77
2	-1	0	1	-1	98.84	79.93
3	0	-1	0	-1	94.33	74.29
4	1	-1	1	-1	96.33	80.65
5	-1	1	0	-1	96.93	65.96
6	0	0	-1	-1	97.94	87.6
7	0	1	1	-1	97.04	82.47
8	1	0	0	-1	95.37	73.24
9	1	1	-1	-1	98.17	89.8
10	0	0	0	-1	97.22	78.29
11	0	0	0	-1	96.34	78.04
12	1	-1	-1	-1	92.53	77.84
13	1	0	1	-1	97.98	83.78
14	-1	-1	0	-1	94.89	79.86
15	0	-1	1	-1	97.93	86.42
16	-1	-1	-1	1	84.54	87.31
17	-1	0	1	1	95.33	82.41
18	0	-1	0	1	88.33	81.72
19	1	-1	1	1	92.38	83.24
20	-1	1	0	1	92.54	82.03
21	0	0	-1	1	90.71	90.54
22	0	1	1	1	97.23	82.26
23	1	0	0	1	91.98	80.83
24	1	1	-1	1	93.33	92.03
25	0	0	0	1	91.83	83.42
26	0	0	0	1	92.18	82.99
27	1	-1	-1	1	86.02	86.34
28	1	0	1	1	95.11	90.68
29	-1	-1	0	1	87.07	84.71
30	0	-1	1	1	93.24	90.51

3.2. Adsorption study of the nanomagnetic adsorbent composite (NMAC)

The design matrix (codified value) and the response value for the percentage of turbidity removal are shown in Table 3. The results showed that NMAC with a particle size less (<) than 45 µm is favorable for the removal of turbidity, whereas CAC with a size greater (>) than 300 µm was better for the removal of turbidity. It might be due to the efficiency of the separation process. Despite their small size, NMAC particles were separated completely during the turbidity test without contaminating recovered water samples. Although Table 3 was not being considered as the response of the full factorial design, it is important to note that the minimum turbidity removal efficiency by NMAC is 84.54% (0.02 g NMAC, 15 mins, 150 rpm, and size of adsorbent >300 µm) which was higher when compared to minimum value resulted by CAC (65.96%) with 0.02g CAC, 60 mins, 200 rpm, and <45 µm of adsorbent.The NMAC adsorption results of this study are similar to Kim (2013) findings, which used iron oxide nanoparticles-impregnated powder activated carbon (IPAC) to remove organic matter from raw water, resulting in a removal efficiency of more than 80%. Therefore, the results show that the presence of high-reactivity iron oxide nanomaterials improves adsorption efficiency.

3.3. Empirical model development for adsorption study

An empirical mathematical model had been generated through a method of steepest ascent and multiple regression analysis of experimental data (Table 3). A predicted response (Y) for turbidity removal efficiency of NMAC and CAC was expressed based on second-order polynomial equation as in Eq (3) and Eq (4), respectively. In the equations, A B, C, and D are coded variables for dosage of adsorbent, time of agitation, rotation speed, and size of adsorbent, respectively. In this study, D (adsorbent size) is a two-level categorical factor that duplicated for every combination of main effect factors (e.g. AABC, ABBC, ABCC). In an area with negligible quadratic effect, categorical factor D=ABC was converted to AB, BD, and CD. BC in the given equation was not converted because it has a 3-level quadratic effect. According to the given equations, the estimated response at the stationary point (center of the system) for NMAC is 94.87; meanwhile, CAC is 82.03. Therefore, it is an estimation that the performance of NMAC in removing turbidity in groundwater is higher than CAC. The negative sign in the equations indicates antagonistic effects; meanwhile, the positive sign indicated synergistic effects. Since the generated empirical equations (Eq. 3 and Eq. 4) are mixed in a positive and negative sign, it shows that the stationary point is a saddle point (Myers *et al.,* 2016). So, the strategy for improving turbidity removal efficiency in the saddle system is flexible (i.e., minimum and maximum range of each variable are considered in optimization process) and depend on the nature of the response system.

$$Y\left[NMAC(\%)\right] = +94.87 + 0.17A + 1.85B + 1.59C + 2.28D - O.39A^2 - 1.82B^2 + 1.33C^2 - 0.31AC - 0.5AD - 1.11BC - 0.68BD - 0.94CD \quad (3)$$

$$Y\left[CAC(\%)\right] = +82.03 + 2.36A - 0.27B - 1.26C + 1.80D - 4.29A^2 - 2.62B^2 + 7.27C^2 + 5.88AB + 1.26AD - 1.25BC - 1.82BD + 0.42CD \quad (4)$$

Table 4 shows the screening of designs based on the analysis of block for second-order models in the form of analysis of variance (ANOVA) generated by Design Expert v.11. The p-values for NMAC and CAC are less than 0.005 which indicates that the model terms are significant. The F-values are compared to identify the fittest model. The highest F-value for NMAC and CAS are quadratic models with 119.34 and 626.26, respectively. This is because of the larger F-value, and the smaller p-value, which denotes the most significant of the corresponding coefficients (Shahmoradi *et al.,* 2018).

Table 4. Sequential model of sum squares for NMAC and CAC

Types of adsorbents	Source	Sum of Squares	df	Mean Square	F-value	p-value
NMAC	Mean vs Total	5.385E+005	1	5.385E+005		
	Block vs Mean	3.19	2	1.59		
	Linear vs Block	484.88	4	121.22	52.89	< 0.0001
	2FI vs Linear	71	6	11.83	10.76	< 0.0001
	Quadratic vs 2FI	46.87	3	15.62	119.34	< 0.0001
	Cubic vs Quadratic	3.03	13	0.23	2.61	0.0135
	Residual	2.86	32	0.089		
	Total	5.391E+005	61	8837.14		
CAC	Mean vs Total	3.98E+05	1	3.98E+05		
	Block vs Mean	179.3	2	89.65		
	Linear vs Block	415.06	4	103.76	3.68	0.0104
	2FI vs Linear	701.16	6	116.86	7.01	< 0.0001
	Quadratic vs 2FI	749.61	3	249.87	626.26	< 0.0001
	Cubic vs Quadratic	6.85	13	0.5272	1.54	0.1619
	Residual	10.3	30	0.3434		
	Total	4.00E+05	59	6785.01		

Table 5. Lack of fit test

Types of adsorbents	Source	Sum of Squares	df	Mean Square	F-value	p-value
NMAC	Linear	122.87	46	2.67	24.07	< 0.0001
	2FI	51.88	40	1.30	11.68	0.0005
	Quadratic	5	37	0.14	1.22	0.4106
	Cubic	1.97	24	0.082	0.74	0.7329
	Pure Error	0.89	8	0.11		
CAC	Linear	1464.14	44	33.28	70.38	< 0.0001
	2FI	762.98	38	20.08	42.47	< 0.0001
	Quadratic	13.37	35	0.3821	0.8082	0.6929
	Cubic	6.52	22	0.2964	0.6268	0.8168
	Pure Error	3.78	8	0.4728		

The lack of fit test is carried out to compare the residual and the pure error. The 'lack of fit F-value' (F_0) for NMAC and CAC (Table 5) are 1.22 and 0.8082, respectively, and their p-values are relatively big. So, we accept the hypothesis that the models adequately describe the data. There are 41.06% (NMAC) and 69.29% (CAC) chance that the 'lack of fit F-value' occurred due to noise. These results imply that a lack of fit for these models was not significant relative to the pure error (Kumar *et al.,* 2018).

3.3.1. Model adequacy

Checking the adequacy of the model is critical to ensure that the empirical models have an adequate approximation to the true system and to verify that the assumptions for square regression are at the point of view (Tezcan *et al.,* 2015). The adequate empirical model must fulfill three residual assumptions, consisting of a normal distribution, constant variance, and independence (Kumar *et al.,* 2018). Normal probability and studentized residual plots of the residuals of NMAC and CAC for removal of turbidity (Figure 2 (a) and (b)) show that most of the points for residual plot concentrated on the central portion of the data, these observations verify that the residuals are normal. Since the results indicate that there are no unusually large residuals, hence, a transformation of the response is not required, which is similar to the findings of Kumar *et al.* (2018).

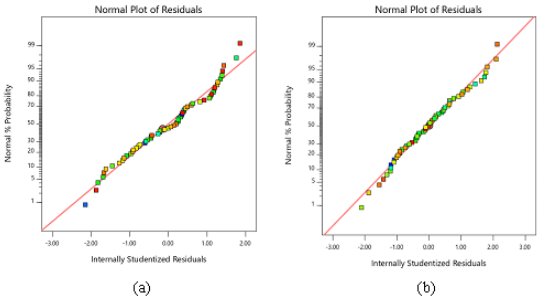

Figure 2. Studentized residual and normal probability plots for removal of turbidity by (a) NMAC and (b) CAC.

Moreover, Figure 3 (a) and (b) show that the residuals are scattered randomly with homoscedasticity. The results reveal that the variance of residuals is constant for all values of y (Tezcan *et al.,* 2015).

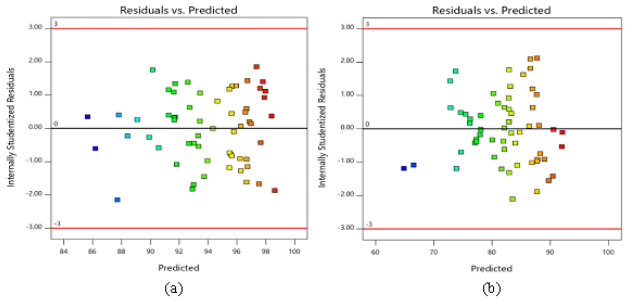

Figure 3. Predicted turbidity removal and studentized residual plots for (a) NMAC and (b) CAC.

Another criterion to indicate the adequacy of the model is the assumption of the independent residual. The assumption will be violated if there is a dependence between residuals which can be observed on negative or positive pattern of the residual plot against time. Based on the observation, there are no discernible pattern of graphs for both NMAC (Figure 4 (a)) and CAC (Figure 4 (b)). So, it is suggested that the residuals are independent (Myers *et al.,* 2016).

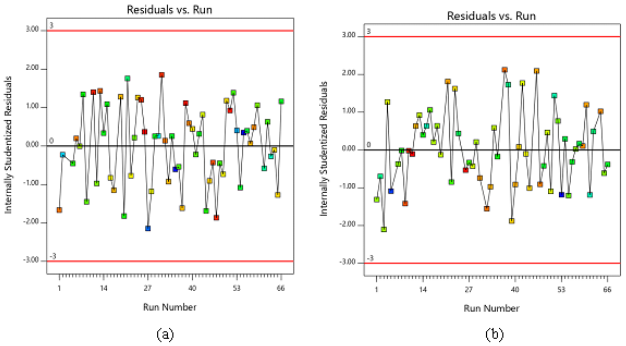

Figure 4. Studentized residual plots by run numbers for (a) nanomagnetic adsorbent composite (NMAC) and (b) commercial activated carbon (CAC).

3.4. Analysis of variance (ANOVA)

The Analysis of variance (ANOVA) (Table 6) investigates the correlation between variables and processing parameters. The analysis reports a 95% confidence interval for model parameters, the dosage of adsorbent, time of agitation, rotation speed, and dosage of adsorbent.

Table 6. Analysis of variance (ANOVA) for NMAC and CAC

Types of adsorbents	Source	Sum of Squares	DF	Mean Square	F Value	Prob > F
NMAC	Block	3.19	2	1.59		
	Model	602.75	13	46.37	354.14	< 0.0001
	A	0.97	1	0.97	7.39	0.0093
	B	114.13	1	114.13	871.72	< 0.0001
	C	75.09	1	75.09	573.55	< 0.0001
	D	297.96	1	297.96	2275.79	< 0.0001
	A2	1.97	1	1.97	15.06	0.0003
	B2	31.34	1	31.34	239.37	< 0.0001
	C2	22.75	1	22.75	173.75	< 0.0001
	AB	0.17	1	0.17	1.32	0.2572
	AC	1.94	1	1.94	14.85	0.0004
	AD	8.13	1	8.13	62.08	< 0.0001
	BC	27.37	1	27.37	209.05	< 0.0001
	BD	16.25	1	16.25	124.09	< 0.0001
	CD	26.25	1	26.25	200.47	< 0.0001
	Residual	5.89	45	0.13		
	Lack of Fit	5	37	0.14	1.22	0.4106
	Pure Error	0.89	8	0.11		
	Cor Total	611.83	60			
CAC	Block	179.3	2	89.65		
	Model	1865.82	13	143.52	359.72	< 0.0001
	A	168.57	1	168.57	422.48	< 0.0001
	B	2.11	1	2.11	5.28	0.0264
	C	46.77	1	46.77	117.21	< 0.0001
	D	177.41	1	177.41	444.65	< 0.0001
	A2	219.16	1	219.16	549.29	< 0.0001
	B2	62.6	1	62.6	156.89	< 0.0001
	C2	622.53	1	622.53	1560.28	< 0.0001
	AB	757.16	1	757.16	1897.71	< 0.0001
	AC	1.16	1	1.16	2.91	0.095
	AD	49.03	1	49.03	122.88	< 0.0001
	BC	32.36	1	32.36	81.11	< 0.0001
	BD	98.75	1	98.75	247.51	< 0.0001
	CD	5.26	1	5.26	13.18	0.0007
	Residual	17.16	43	0.4		
	Lack of Fit	13.37	35	0.38	0.81	0.6929
	Pure Error	3.78	8	0.47		
	Cor Total	2062.28	58			

However, there are non-significant terms (Table 6) for NMAC (AB; p-value > 0.05) and CAC (AC; p-value > 0.05). As a result, the identified terms were dropped in the empirical model resulting in the formation of reduced quadratic model for the process (Eq. 3 and Eq. 4). It is important to drop the non-significant terms as there are differences between full and reduced model in predicted error sum of squares (PRESS) and Adjusted R-Squared (Table 7). The reduced quadratic model in this study is in agreement with Shahmoradi *et al.* (2018) findings that the generated empirical models is better satisfied after dropping non-significant terms. The analysis is considered to support the generated empirical models and are good because more than half of the terms in ANOVA are significant (Shahmoradi *et al.,* 2018).

3.5. Effect of adsorption parameters

The perturbation plot is used to investigate changes in responses as each individual factor moves from the selected reference point while the other factors at the reference value are held constant. The reference point is the coded zero level in the middle of the design space. A steep slope in the results suggest the sensitivity of a response to a factor. As far as the slope was concerned, positive coefficient was pushed up while negative coefficient was pressed down (Anderson & Whitcomb, 2017). The studied factors include dosage of adsorbent (A), time of agitation (B), rotation speed (C), and size of adsorbent (D). The perturbation plots for NMAC with size of adsorbent < 45 µm and > 300 µm are represented in Figure 5 (a) and (b) respectively. The perturbation plot for

NMAC (Figure 5 (a) and (b)) show that factor A (dosage of adsorbent) produces relatively flat line. So, it is suggested that dosage of adsorbent (A) was sensitive to turbidity removal efficiency but the lowest influence on removal process. Meanwhile the steepest curve of factor B (time of agitation) and C (rotation speed) indicate that turbidity removal efficient is sensitive to time and rotation speed. The research found that turbidity removal efficiency among different dosages of NMAC (0.02, 0.04, and 0.06 g) showed relatively small difference. This might be due to the presence of iron oxide nanomaterials on the surface of adsorbent which improves activation of the pores. Besides, another reason is likely because of the process of separating NMAC from groundwater, which is aided by external magnetic field. The efficient separation process to separate NMAC regardless of the amount of dosage resulted in clean water without leaving any adsorbent residues in the groundwater sample. When compared to the perturbation plots for CAC with the size of adsorbent < 45 µm and > 300 µm in Figure 5 (c) and (d), respectively, factor B (time of agitation) shows relatively small effect as it moved from the reference point. Factor C (rotation speed) shows the steepest curve in both Figure (5 (c)) and (d). Hence, it indicates that turbidity removal is insensitive to time of agitation (B) but sensitive to rotation speed (C). The role of factor A (dosage of adsorbent) is dynamic between two ranges of adsorbent size. The turbidity removal efficiency is more sensitive to dosage of adsorbent with larger size (> 300 µm). Turbidity removal efficiency is relatively insensitive towards time of agitation, this might be due to rapid adsorption. Apart from that, separation efficiency is weak for CAC. Since CAC does not have magnetic properties, the separation of CAC by using filter paper might leave some adsorbent residues in the groundwater sample. Thus, even though the adsorption is well at the given time of agitation, the inefficient separation causes drawback on quality of treated groundwater.

Table 7. Comparison between full quadratic and reduced quadratic model for NMAC and CAC

Sources	NMAC		CAC	
	Full quadratic model	Reduced quadratic model	Full quadratic model	Reduced quadratic model
Std.Dev	0.36	0.36	0.63	0.65
Mean	93.95	93.95	82.16	82.16
CV	0.39	0.39	0.77	0.79
PRESS	11.68	11.32	34.46	35.35
R-Squared	0.9903	0.9900	0.9909	0.9903
Adj R-Squared	0.9875	0.9874	0.9881	0.9876
Pred R-Squared	0.9808	0.9814	0.9817	0.9812
Adeq Precision	70.049	72.204	82.74	84.349

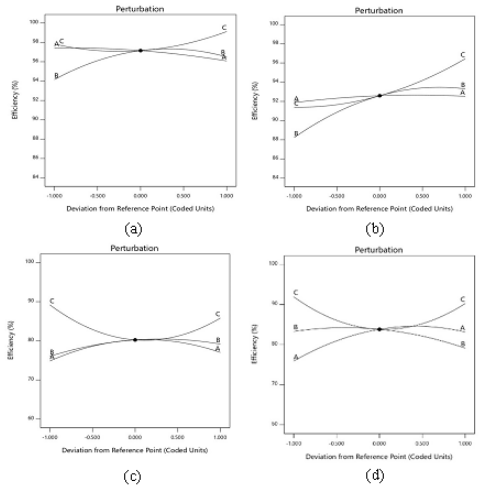

Figure 5. Perturbation plots for turbidity removal efficiency for (a) NMAC with size < 45 µm, (b) NMAC with size > 300 µm, (c) CAC with size < 45 µm, and (d) CAC with size > 300 µm.

3.5.1. Optimization

The empirical model generated graphs of 3D response surface and 2D contour plots to portray the interaction between independent and dependent variables. The significance of the interactions is indicated by elliptical shape, whereas the circular shape indicates insignificant interaction. The 3D response surface and contour plots (Figure 6 (a)) shows the interaction between dosage of adsorbent (A) and rotation speed (C) for NMAC. The increase in the dosage of adsorbent from 0.02 g to 0.04 g improves turbidity removal efficiency. The decline in turbidity removal efficiency occurred when the dosage of adsorbent is over 0.04 g, and there is no obvious effect when rotation speed is over 150 rpm. The turbidity removal efficiency decreased at a relatively high rotation speed as molecules in turbid raw water and adsorbent are hastily colliding with each other and lead to detachment of loosely bound impurities molecule (Latinwo *et al.,* 2019). The results shown in Figure 6 (b) indicates that the optimum turbidity removal time by NMAC lies between 24 min to 33 min. Increment in time of agitation may improve turbidity removal efficiency, but it does not show any obvious effect as rotation speed increases. The rapid adsorption may occur due to diffusion control from the bulk of the liquid phase to the unoccupied binding site at the surface of the adsorbent (Latinwo *et al.,* 2019). In accordance with the present results, the previous study by Liang (2018) concurred that rapid sorption of contaminants occurs at the initial rate and occupied sites of $CoFe_2O_4$/AC, resulting in the sorption to decrease at a later stage.

Figure 7 (a) exhibits the relationship between the dosage of adsorbent and time of agitation on turbidity removal efficiency of CAC. The increment of the dosage of adsorbent along with time improves turbidity removal

efficiency. However, the removal efficiency declined as the dosage of adsorbent exceeded 0.04 g, and the time of agitation was beyond 24 min to 33 min. Slow adsorption occurs at a later stage occur as a result of the smaller available site for adsorption (Sivaprakasam & Venugopal, 2019), and this limitation might occur because iron oxide nanomaterials are not present on the surface of CAC. Moreover, the interaction between time of agitation and rotation speed in Figure 7 (b) depicts that optimum turbidity removal efficiency lies in the range 24 to 33 min and 190 rpm to 210 rpm. Turbidity that is due to solutes that reduce the surface tension of water can be easily taken up by the adsorbent (CAC). The high rate of a collision results in high adsorption. However, physical adsorption involves weak van der Walls force (Patterson, 2009). So, it is likely to affect turbidity removal efficiency during the later stages at rotation speed of above 210 rpm.

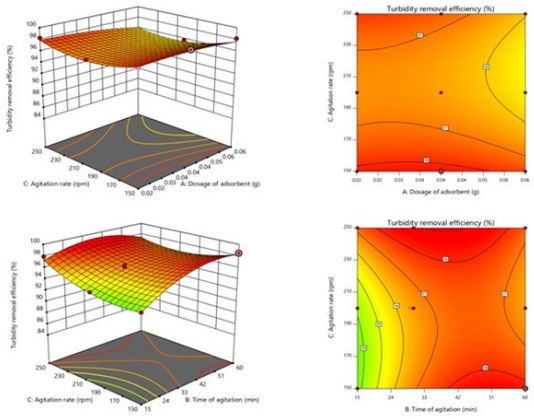

Figure 6. 3D Response surface and 2D contour plots for speed of agitation and dosage of NMAC for the interaction of: (a) dosage of adsorbent and rotation speed (AC) and (b) time of agitation and rotation speed (BC).

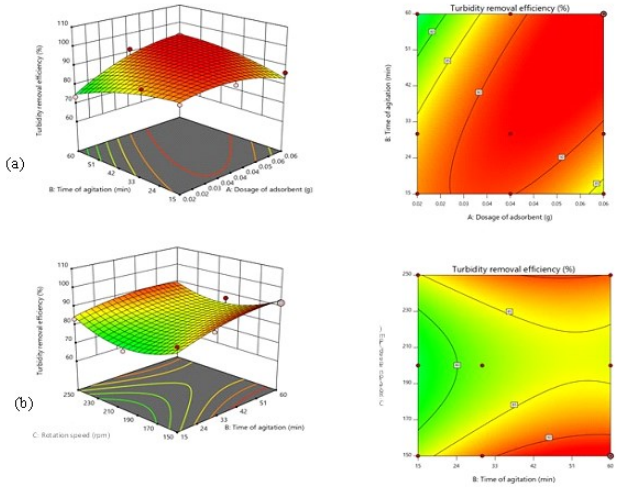

Figure 7. 3D Response surface and 2D contour plots for speed of agitation and dosage of CAC for the interaction of (a) dosage of adsorbent and agitation time (AB) and (b) time of agitation and rotation speed (BC).

3.6. Verification of the predictive model

The optimization experiment is conducted to identify optimum conditions for maximum turbidity removal efficiency. Table 8 shows the generated optimum condition by Design Expert 11 and actual results gathered for NMAC and CAC, respectively. The readings show that turbidity removal efficiency by NMAC is 98.76% (0.40 NTU), whereas the performance of CAC is 84.84% (3.07 NTU). So, the treated groundwater complies with the Malaysia drinking water standard, which is below 5 NTU. The results reveal that the actual value turbidity removal efficiency by NMAC is 0.26% higher than the predicted value. Also, the actual value for turbidity removal efficiency by CAC is 0.21% higher than predicted value. Overall, the results indicated that the optimization parameters are reliable with no significant differences between predicted and actual results.

Table 8. Optimized parameters with predicted and actual value for turbidity removal efficiency by both NMAC and CAC

Types of adsorbents	Condition	Turbidity removal efficiency (%)	Dosage of adsorbent (g)	Time of agitation (min)	Rotation speed (rpm)	Size of adsorbent (µm)
NMAC	Predicted	98.50	0.04	48	150	<45
	Actual	98.76	0.04	48	150	<45
CAC	Predicted	84.66	0.03	22	250	<45
	Actual	84.84	0.03	22	250	<45

4. Conclusion

Nanomagnetic adsorbent composite (NMAC) was used for adsorption study for turbidity removal of groundwater and commercial activated carbon (CAC) as a standard reference for comparison. RSM was adopted in the study to optimize turbidity removal efficiency factors. Model adequacy analysis revealed that the generated quadratic model fits the experiment carried out. From the derived quadratic model for turbidity removal efficiency and analysis of variance, 0.93% of adsorbent dosage (NMAC) and 2.64% of agitation time for CAC were considered as high compared to other extreme values in Table 6 (>0.0000001). Although the p-values of main effects (adsorbent dosage (NMAC) and agitation time (CAC)) are less than 0.05, the obtained values were closer to calculated null hypothesis compared to other reported main effects (Table 6). The results show the crucial role of iron oxide nanomaterial adsorbent composite in turbidity removal from raw water. The optimum NMAC process parameters were 0.04 g adsorbent dose, 45 µm adsorbent size, 48 min agitation at 150 rpm rotation speed. The test showed that the optimal parameters were accurate and that NMAC's performance was 14% higher than CAC for optimal turbidity removal efficiency. Consequently, for subsequent stage of scaling up, the created empirical model from a 3k factorial design

is useful and that NMAC is a competitive adsorbent to treat water efficiently compared to CAC.

Acknowledgment

The authors acknowledge financial support from Universiti Malaysia Kelantan Research Fund (R/PRO/A07.00/01397A/008/2021/00975) and (R/SGJP/A07.00/01397A/005/2018/0057).

References

Anderson M.J. and Whitcomb P.J. (2017), *RSM Simplified*. *CRC Press* (2th.)

Awang H., Abdullah P.S., Wen L., Ling H.Y., Barasarathi J., & Azmin S.N.H.M. (2022). Raw Water Treatment from Selected Areas In Kelantan Using Coconut Shell Derived Nanomagnetic Adsorbent Composite (CS-NMAC). Journal of Sustainability Science and Management, 17(2), 77–90.

Ayob.N.A.F.C., and Musa.S.(2022). Frequency Analysis on Groundwater Consumption and Water Billed to the Community in Kelantan. In IOP Conference Series: Earth and Environmental Science (Vol. 1022, No. 1, p012073). IOP Publishing.

Basrur D., and Ishwara B.J.(2019)An investigation on the characterization of activated carbon from areca leaves and their adsorption nature towards different dyes, *Global NEST Journal*, **21**(2), 124–130.

Crini G., Lichtfouse E., Wilson L.D. and Morin N. (2018), Conventional and non-conventional adsorbents for wastewater treatment, *Environmental Chemistry Letters,* **17**(1), 195–213.

Hazimah H.H., Mohamad R., Nurhidayu S., Zulfa H.A. and Faradiella M.K. (2019), Hydrogeochemistry investigation on groundwater in Kuala Langat, Banting, Selangor, *Bulletin of the Geological Society of Malaysia*, **67**, 127–134.

Hidayu A.R., Mohamad N.F., Matali S. and Sharifah A.S.A.K. (2013), Characterization of activated carbon prepared from oil palm empty fruit bunch using BET and FT-IR techniques, *Procedia Engineering*, **68**, 379–384.

Huda A., Palsan S.A., & ZulAriff A.L. (2020). A preliminary study of local behaviour, perceptions & willingness to pay towards better water. In IOP Conference Series: Earth and Environmental Science (pp. 1–10).

Karthikeyan S., Sivakumar P. and Palanisamy P.N. (2008), Novel Activated Carbons from Agricultural Wastes and their Characterization, *E-Journal of Chemistry*, **5**, 409-426.

Kumar S., Meena H., Chakraborty S. and Meikap B.C. (2018), Application of response surface methodology (RSM) for optimization of leaching parameters for ash reduction from low-grade coal, *International Journal of Mining Science and Technology*, **28**(4), 621-629.

Latinwo G.K., Alade A.O., Agarry S.E. and Dada E.O. (2019), Process Optimization and Modeling the Adsorption of Polycyclic Aromatic-Congo Red Dye onto Delonix regia Pod-Derived Activated Carbon, *Polycyclic Aromatic Compounds*, **3**(1), 38-45.

Liang Y., He Y., Wang T. and Lei L. (2019), Adsorptive removal of gentian violet from aqueous solution using $CoFe_2O_4$ / activated carbon magnetic composite, *Journal of Water Process Engineering*, **27**, 77-88.

Liu Z., Wei H., Li A. and Yang H. (2018), Enhanced coagulation of low-turbidity micro-polluted surface water: Properties and optimization, *Journal of Environmental Management*, **233**,739-747.

Meng P., Fang X., Maimaiti A., Yu G. and Deng S. (2019), Efficient removal of perfluorinated compounds from water using a regenerable magnetic activated carbon, *Chemosphere*, **224**, 187-194.

Milne T.A., Chum H.L., Agblevor F.A. and Johnson D.K. (1992), "Standardized Analytical Methods' Biomass & Bioenergy, *Proceedings of International Energy Agency Bioenergy Agreement Seminar*, **2**(1–6), 341-366.

Ministry of Health Malaysia. (2014), Drinking Water Quality Standards and Frequency of Monitoring. Retrieved December 7, 2019, from http://kmam.moh.gov.my/public-user/drinking-water-quality-standard.html.

Mohd F.F.R. and Noorazuan M. (2018), Perubahan Kualiti Air Bawah Tanah di Negeri Kelantan Pada Tahun 2010 Hingga 2012, *Jurnal Wacana Sarjana*, **2**(2), 1-10.

Muoio R., Caretti C., Rossi L., Santianni D. and Lubello C. (2020), International Journal of Hygiene and Water safety plans and risk assessment: A novel procedure applied to treated water turbidity and gastrointestinal diseases, *International Journal of Hygiene and Environmental Health*, **223** (1), 281-288.

Myers R.H., Montgomery D.C. and Anderson C.C.M. (2016), Response Surface Methodology (4th.), New Jersey: John Wiley & Sons, Inc.

Park W., Jeong S., Im S. and Jang A. (2020), High turbidity water treatment by ceramic microfiltration membrane: Fouling identification and process optimization, *Environmental Technology & Innovation*, **17**, 100578.

Patterson H.B.W. (2009), Adsorption, In *Bleaching and Purifying Fats and Oils Theory and Practice* Elsevier Inc.

Santhosh C., Malathi A., Dhaneshvar E., Bhatnagar A., Grace A.N. and Madhavan J. (2019), *Chapter 16 - Iron Oxide Nanomaterials for Water Purification*. *Nanoscale Materials in Water Purification*. Elsevier Inc.

Shahmoradi B., Yavari S., Zandsalimi Y., Shivaraju H.P., Negahdari M., Maleki A., Mckay G., Radheshyam R.P. and Lee S.M. (2018), Optimization of solar degradation efficiency of bio-composting leachate using Nd: ZnO nanoparticles, *Journal of Photochemistry and Photobiology A: Chemistry*, **356***,* (1), 201–211.

Sivaprakasam A. and Venugopal T. (2019), Modelling the removal of lead from synthetic contaminated water by activated carbon from biomass of *Diplocyclos Palmatus* by RSM, *Global NEST Journal*, **21**(3), 319–327.

Sun H., Yang B. and Li A. (2019), Biomass derived porous carbon for efficient capture of carbon dioxide, organic contaminants and volatile iodine with exceptionally high uptake, *Chemical Engineering Journal*, **372**(4), 65–73.

Tancredi P., Veiga L.S., Garate O. and Ybarra G. (2019), Magnetophoretic mobility of iron oxide nanoparticles stabilized by small carboxylate ligands, *Colloids and Surfaces A*, **579**(5), 123664.

Tezcan Un U., Ates F., Erginel N., Ozcan O. and Oduncu E. (2015), Adsorption of Disperse Orange 30 dye onto activated carbon derived from Holm Oak (Quercus Ilex) acorns: A 3k factorial design and analysis, *Journal of Environmental Management*, **155**, 89–96.

Wannahari R., Sannasi P., Nordin M.F.M. and Mukhtar H. (2018) Sugarcane Bagasse Derived Nano Magnetic Adsorbent Composite (Scb-Nmac) for Removal of Cu^{2+} From Aqueous

Solution, *ARPN Journal of Engineering and Applied Sciences*, **13**(1), 1–9.

World Health Organization (WHO) 2022. Groundwater, invisible but vital to health. Retrieved July 7, 2022, from https://www.who.int/news-room/feature-stories/detail/world-water-day-2022-groundwater-invisible-but-vital-to-health.

Yong C.Z., Denys P.H., Pearson C.F. and Pearson C.F. (2018), Groundwater extraction-induced land subsidence: a geodetic strain rate study in Kelantan, Malaysia strain rate study in Kelantan, Malaysia, *Journal of Spatial Science*, **8596**, 1–12.

Zainol N.F.M., Zainuddin A.H., Looi L.J., Aris A.Z., Isa N.M., Sefie A., Ku Yusof K.M.K. (2021). Spatial Analysis of Groundwater Hydrochemistry through Integrated Multivariate Analysis: A Case Study in the Urbanized Langat Basin, Malaysia. Int J Environ Res Public Health. 27;18(11):5733.

Zhu Z., Huang C.P., Zhu Y., Wei W. and Qin H. (2018), A hierarchical porous adsorbent of nano- α -Fe_2O_3 / Fe_3O_4 on bamboo biochar (HPA-Fe / C-B) for the removal of phosphate from water, *Journal of Water Process Engineering*, **25**, (4), 96–104.

Zulkania A., F G.H. and Rezki A.S. (2018), The potential of activated carbon derived from bio-char waste of bio-oil pyrolysis as adsorbent, *MATEC*, *01029*, 1–6.